Inhibition of Alanine:Glyoxylate Aminotransferase 1 Dimerization Is a Prerequisite for Its Peroxisome-to-Mitochondrion Mistargeting in Primary Hyperoxaluria Type 1

James M. Leiper, Paru B. Oatey, and Christopher J. Danpure

Medical Research Council Laboratory for Molecular Cell Biology and Department of Biology, University College London, London WC1E 6BT, United Kingdom

Abstract. Peroxisome-to-mitochondrion mistargeting of the homodimeric enzyme alanine:glyoxylate aminotransferase 1 (AGT) in the autosomal recessive disease primary hyperoxaluria type 1 (PH1) is associated with the combined presence of a normally occurring $Pro_{11}Leu$ polymorphism and a PH1-specific $Gly_{170}Arg$ mutation. The former leads to the formation of a novel NH_2-terminal mitochondrial targeting sequence (MTS), which although sufficient to direct the import of in vitro–translated AGT into isolated mitochondria, requires the additional presence of the $Gly_{170}Arg$ mutation to function efficiently in whole cells. The role of this mutation in the mistargeting phenomenon has remained elusive. It does not interfere with the peroxisomal targeting or import of AGT. In the present study, we have investigated the role of the $Gly_{170}Arg$ mutation in AGT mistargeting. In addition, our studies have led us to examine the relationship between the oligomeric status of AGT and the peroxisomal and mitochondrial import processes. The results obtained show that in vitro–translated AGT rapidly forms dimers that do not readily exchange subunits. Although the presence of the $Pro_{11}Leu$ or $Gly_{170}Arg$ substitutions alone had no effect on dimerization, their combined presence abolished homodimerization in vitro. However, AGT containing both substitutions was still able to form heterodimers in vitro with either normal AGT or AGT containing either substitution alone. Expression of various combinations of normal and mutant, as well as epitope-tagged and untagged forms of AGT in whole cells showed that normal AGT rapidly dimerizes in the cytosol and is imported into peroxisomes as a dimer. This dimerization prevents mitochondrial import, even when the AGT possesses an MTS generated by the $Pro_{11}Leu$ substitution. The additional presence of the $Gly_{170}Arg$ substitution impairs dimerization sufficiently to allow mitochondrial import. Pharmacological inhibition of mitochondrial import allows AGT containing both substitutions to be imported into peroxisomes efficiently, showing that AGT dimerization is not a prerequisite for peroxisomal import.

BOTH mitochondrial and peroxisomal precursor proteins are synthesized on free polyribosomes in the cytosol and are imported posttranslationally into their respective organelles (17, 25). Despite these similarities, many studies suggest that the targeting information and structural requirements for mitochondrial and peroxisomal protein import are very different. Most mitochondrial precursor proteins are synthesized with NH_2-terminal extensions, which are cleaved after mitochondrial import (1, 13). Targeting information in the presequence is determined by secondary rather than primary structure. In particular, the ability to form positively charged amphipathic α helices appears to be crucial (28, 36). It is widely accepted that mitochondrial precursor proteins must be maintained in a partially unfolded monomeric state to be translocated across the mitochondrial membrane (8, 29). Indeed, mitochondrial proteins that do assume a folded configuration in the cytosol appear to be unfolded during import (3, 8). Conversely, tightly folded and disulfide bonded proteins or large oligomeric complexes are not competent for import into mitochondria (3, 8).

Please address all correspondence to Dr. C.J. Danpure, Medical Research Council Laboratory for Molecular Cell Biology, University College London, Gower Street, London WC1E 6BT, United Kingdom. Tel.: 44-171-380-7936; Fax: 44-171-380-7936; E-mail: c.danpure@ucl.ac.uk

Two types of peroxisomal targeting sequences (PTSs)[1] have been identified within mammalian peroxisomal matrix proteins (30). The first to be characterized (PTS1) consists of a COOH-terminal tripeptide with a consensus S(A,C)-K(R,H)-L(M) (12, 32). This motif is found in many peroxisomal matrix proteins and is not cleaved after import. The second mammalian PTS (PTS2), which so far has only been identified in 3-ketoacyl-CoA thiolase, consists of a cleavable NH_2-terminal sequence of 26 or 36 amino acids (depending on species) with a consensus motif of X_n-RL-X_5-HL-X_n (24, 31). It should be noted, however, that many peroxisomal matrix proteins do not appear to contain either a PTS1 or PTS2 sequence, as defined above.

In contrast to mitochondrial precursors, many peroxisomal proteins are capable of productive folding and oligomerization in the cytosol. For example, the peroxisomal protein firefly luciferase (FFL) is efficiently folded when synthesized in reticulocyte lysates in vitro (14). Also, in cells from patients with a defect in the import of PTS1-containing proteins, the peroxisomal enzyme catalase appears to assemble into catalytically active tetramers in the cytosol (20). More recent studies have provided evidence that cytosolically assembled protein oligomers can be translocated across the peroxisomal membrane of yeast. Thus, homodimers of yeast thiolase and homotrimers of bacterial chloramphenicol acetyltransferase (CAT) fused to a PTS1 can be translocated across the peroxisomal membrane of *Saccharomyces cerevisiae* without previous disassembly (10, 18). Further evidence supporting a mechanism of translocation that can accommodate large oligomeric protein complexes has been provided by the work of Walton et al., who have demonstrated that 4–9-nm colloidal gold particles coated with a human serum albumin (HSA)–PTS1 peptide conjugate can be imported into peroxisomes after microinjection into human fibroblasts in culture (37).

In humans, the liver-specific enzyme alanine:glyoxylate aminotransferase 1 (AGT) is localized to the peroxisomal matrix, where it exists as a homodimer (5, 22). The PTS of AGT has yet to be completely defined. Although recent studies have indicated that AGT is imported via the PTS1-dependent pathway, the COOH terminus of human AGT (KKL) does not fit the previously defined PTS1 consensus. Despite the COOH-terminal tripeptide of AGT being necessary for targeting, it has been shown to be insufficient to direct the peroxisomal import of the bona fide peroxisomal matrix protein FFL and the bacterial reporter protein CAT (21). These observations have led to the suggestion that the PTS1 of AGT is more complex than a simple COOH-terminal tripeptide. In a subset of patients with the rare autosomal recessive disorder primary hyperoxaluria type 1 (PH1), disease results from the mislocalization of AGT to mitochondria rather than to peroxisomes (6). Previously, we have demonstrated that mistargeting of AGT in these individuals is associated with the combined presence of two normally occurring polymorphisms, Pro_{11}Leu and Ile_{340}Met, and a PH1-specific Gly_{170}Arg mutation (27). The Pro_{11}Leu substitution was predicted to greatly enhance the likelihood of the NH_2-terminal region of AGT folding as a positively charged amphiphilic α-helix that might then function as an MTS. Indeed, in isolated mitochondrial import assays, the Pro_{11}Leu substitution alone was shown to be sufficient for the import of at least a small proportion of in vitro–translated AGT, while Gly_{170}Arg and Ile_{340}Met were neither necessary nor sufficient for mitochondrial import (26). In whole cells, however, both Pro_{11}Leu and Gly_{170}Arg are necessary for significant mitochondrial import, although neither is sufficient alone (21, 27). Ile_{340}Met was neither necessary nor sufficient. Since neither Pro_{11}Leu nor Gly_{170}Arg amino acid substitutions interfere with peroxisomal import (21), the role of the Gly_{170}Arg mutation in the peroxisome-to-mitochondrion mistargeting of AGT has remained enigmatic.

In this paper, we have attempted to resolve this issue. The results presented show that normal AGT is imported into peroxisomes as a dimer, although dimerization is not a prerequisite for peroxisomal import. On the other hand, mutant AGT can only be imported into mitochondria as a monomer. The peroxisome-to-mitochondrion mistargeting of AGT in PH1 is, therefore, caused by the combined effects of (*a*) the generation of an MTS caused by the Pro_{11}Leu polymorphism; and (*b*) the inhibition of dimerization caused by the combined presence of the Pro_{11}Leu polymorphism and the Gly_{170}Arg mutation. This is not only the first demonstration of the peroxisomal import of a naturally occurring oligomeric PTS1 protein, but also the first demonstration that oligomerization can determine, at least in part, the intracellular fate of a protein.

Materials and Methods

Construction of Expression Plasmids

The various AGT expression plasmids used in this study are described in Table I. The construction of plasmids encoding normal human AGT, the various mutant forms of human AGT (AGT^A, AGT^B, AGT^{AB}, AGT^{ABC}, and AGTΔ1), and FFL in the in vitro expression vector pBluescriptKS$^+$ and the mammalian expression vector pHYK have been described previously (21, 26). To produce COOH-terminal, myc epitope–tagged derivatives of these AGT constructs, normal human AGT was PCR amplified with the top-strand primer CTTCTCCTTCTACCTGGACA and the bottom-strand primer CGGATCGGATCCTCA**CAGGTCCTCCTCGGAGATCAGCTTCTGCTC**GCCGCC*CTTGGGGCAGTGCTG*. The 3′ end of the bottom-strand primer (italicized) is complementary to basepairs 1289–1275 of human AGT cDNA and then encodes two glycine residues followed by the 10-amino acid c-*myc* epitope (bold), a stop codon, and a BamHI restriction site (underlined). The top-strand primer is complementary to basepairs 833–852 of human AGT cDNA and is upstream of a unique ApaI restriction site (basepair 1180) in the cDNA. The PCR product was digested with ApaI and BamHI, and was cloned into the appropriate ApaI- and BamHI-digested plasmids to generate each of the myc-tagged plasmids described in Table I. Thus, in each myc-tagged AGT construct, the COOH-terminal PTS1 tripeptide has been replaced with two glycine residues followed by the myc epitope (EQKLISEEDL). All sequences generated by PCR were sequenced.

In Vitro Transcription and Translation

For in vitro transcription, ~1 μg of plasmid DNA was linearized with BamHI before transcription with T3 RNA polymerase (Promega, Southampton, UK) according to the manufacturer's instructions. Aliquots of in vitro transcription reactions (1 μl and ~1 μg of RNA) were used directly

1. *Abbreviations used in this paper*: AGT, alanine:glyoxylate aminotransferase 1; BS3, bis (sulfosuccinimidyl) suberate; CAT, chloramphenicol acetyltransferase; CCCP, carbonyl cyanide *m*-chlorophenylhydrazone; FFL, firefly luciferase; HSA, human serum albumin; MTS, mitochondrial targeting sequence; PBSA, phosphate-buffered saline A; PH1, primary hyperoxaluria type 1; PTS, peroxisomal targeting sequence.

Table I. Description of the AGT Expression Plasmids Used in This Study

Plasmid	Previous name*	Description
AGT	AGT^{a}/AGT^{pgi}	Normal AGT encoded by the major allele
AGT^{A}	AGT^{lgi}	AGT containing a $Pro_{11}Leu$ substitution
AGT^{B}	AGT^{pri}	AGT containing a $Gly_{170}Arg$ substitution
AGT^{AB}	AGT^{lri}	AGT containing both $Pro_{11}Leu$ and $Gly_{170}Arg$ substitutions
AGT^{ABC}	AGT^{lrm}	AGT containing $Pro_{11}Leu$, $Gly_{170}Arg$, and $Ile_{340}Met$ substitutions
AGTΔ1	$AGT^{a}\Delta1$	COOH-terminal KKL of normal AGT deleted
AGT-myc		COOH-terminal KKL of AGT replaced with c-*myc* epitope
AGT^{A}-myc		COOH-terminal KKL of AGT^{A} replaced with c-*myc* epitope
AGT^{B}-myc		COOH-terminal KKL of AGT^{B} replaced with c-*myc* epitope
AGT^{AB}-myc		COOH-terminal KKL of AGT^{AB} replaced with c-*myc* epitope
AGT^{ABC}-myc		COOH-terminal KKL of AGT^{ABC} replaced with c-*myc* epitope

For expression in vitro, each of the cDNA constructs was cloned into pBluescriptIIKS^{+}. For expression by transfection in whole cells, the constructs were cloned into the mammalian expression vector pHYK.
*The previous names are those used in reference 21.

for in vitro translation in reticulocyte lysates (Promega) containing [^{35}S]L-methionine (NEN Dupont, Stevenage, UK) following the manufacturer's instructions for 40 min at 30°C.

Preparation of Liver Homogenates

Approximately 0.5 g of frozen human liver was finely sliced and suspended in 5 ml of ice-cold phosphate-buffered saline A (PBSA) and homogenized by five passes through a tight-fitting glass/Teflon motor-driven homogenizer. The homogenate was centrifuged at 25,000 *g* for 30 min at 4°C. The supernatant was retained and diluted with ice-cold PBSA to a concentration of 5 μg protein/ml.

Chemical Cross-linking

The water-soluble homobifunctional cross-linker bis (sulfosuccinimidyl) suberate (BS3; Pierce, UK) was used to cross-link AGT in various fractions as follows:

In Vitro–translated AGT. Aliquots of translation reactions (5 μl) were diluted fivefold in cross-linking buffer (100 mM potassium phosphate, pH 7.4) containing 1 mM BS3, and were incubated for 30 min at room temperature. Cross-linking was terminated by the addition of 1 μl of 1 M Tris/HCl, pH 7.4. Aliquots (5 μl) of cross-linking reactions were analyzed by SDS-PAGE followed by fluorography. Where indicated, translation reactions were treated with 150 mU of potato apyrase (Sigma, Poole, UK) for 30 min at 30°C before cross-linking to deplete ATP from the reticulocyte lysate.

AGT in Human Liver Homogenates. Aliquots (5 μl and ~25 μg of protein) of liver homogenates were diluted fivefold in cross-linking buffer containing BS3 at the concentrations indicated. Reactions proceeded for 30 min at room temperature and were terminated by the addition of 1 μl of 1 M Tris/HCl, pH 7.4. Aliquots of reactions were resolved by SDS-PAGE, transferred to nitrocellulose membranes, and analyzed by immunoblotting with rabbit anti–human AGT polyclonal antisera, followed by an HRP-conjugated goat anti–rabbit IgG (Sigma) and visualization by enhanced chemiluminescence (ECL; Amersham International, Amersham, UK).

Purified Human AGT. Approximately 2 μg of purified normal human AGT was diluted into 25 μl of cross-linking buffer and cross-linked with BS3 at the concentrations indicated. After termination of cross-linking, reactions were resolved by SDS-PAGE, and AGT was visualized by silver staining.

Immunoprecipitation

For immunoprecipitation of in vitro–translated proteins, 15-μl aliquots of reactions were diluted into 300 μl of immunoprecipitation buffer (150 mM NaCl, 1 mM EDTA, 0.1% Triton X-100, 50 mM Tris/HCl, pH 8.0) and precleared by incubation with 5 μg of preswollen protein A–Sepharose (Sigma) for 1 h at 4°C. Samples were then centrifuged for 1 min at 13,000 rpm in a microfuge to pellet the protein A–Sepharose. The supernatants were removed and incubated for 2 h at 4°C with 20 μl of tissue culture medium containing the mouse anti-myc mAb 9E10 (~2 mg protein/ml). Antibody/antigen complexes were then precipitated by adding 5 μg of preswollen protein A–Sepharose and incubating for 1 h at 4°C. Protein A–Sepharose was collected by centrifugation, and the pellets washed five times in 300 μl of immunoprecipitation buffer. Proteins were eluted from washed pellets by boiling in 30 μl of sample loading buffer (125 mM Tris/HCl, 2% SDS [wt/vol], 5% β-mercaptoethanol [vol/vol], 20% glycerol [wt/vol], 0.0025% bromophenol blue [wt/vol], pH 6.8), resolved by SDS-PAGE, and visualized by fluorography.

Cell Culture and Transfection

SV-40–transformed monkey kidney cells (COS-1) were grown in DME

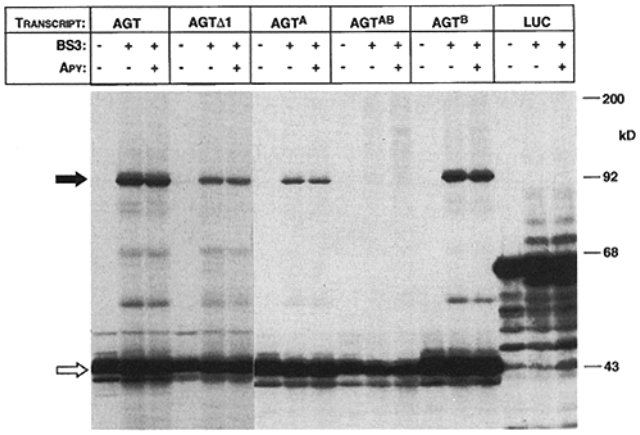

Figure 1. Chemical cross-linking of in vitro–translated AGT. Aliquots of in vitro translation reactions, programmed with transcripts encoding the proteins indicated, were either cross-linked with the chemical cross-linker BS3 (+BS3) or uncross-linked (-BS3). For descriptions of AGT, AGTΔ1, AGT^{A}, AGT^{B}, and AGT^{AB}, see Table I. Firefly luciferase (*LUC*) was used as a control. Where indicated, endogenous ATP was depleted from lysates before cross-linking by incubation with apyrase (+/− *Apy*). After cross-linking, samples were resolved by SDS-PAGE on 8% gels, and the [^{35}S]L-methionine–labeled in vitro–translated proteins were visualized by fluorography. The migration position of monomeric AGT (*open arrow*) and the ~90-kD AGT cross-linking product (*filled arrow*) are indicated. Positions of the molecular mass markers (in kilodaltons) are shown on the right-hand side. Although the intensities of the 90-kD cross-linked products vary between the different AGT constructs, with the exception only of AGT^{AB}, they are proportional to the intensities of the respective uncross-linked monomers. Therefore, this variation probably results from different translation efficiencies rather than from any differences in the efficiencies of cross-linking. No 90-kD product was apparent when AGT^{AB} was cross-linked, even on longer exposures of the autoradiograms.

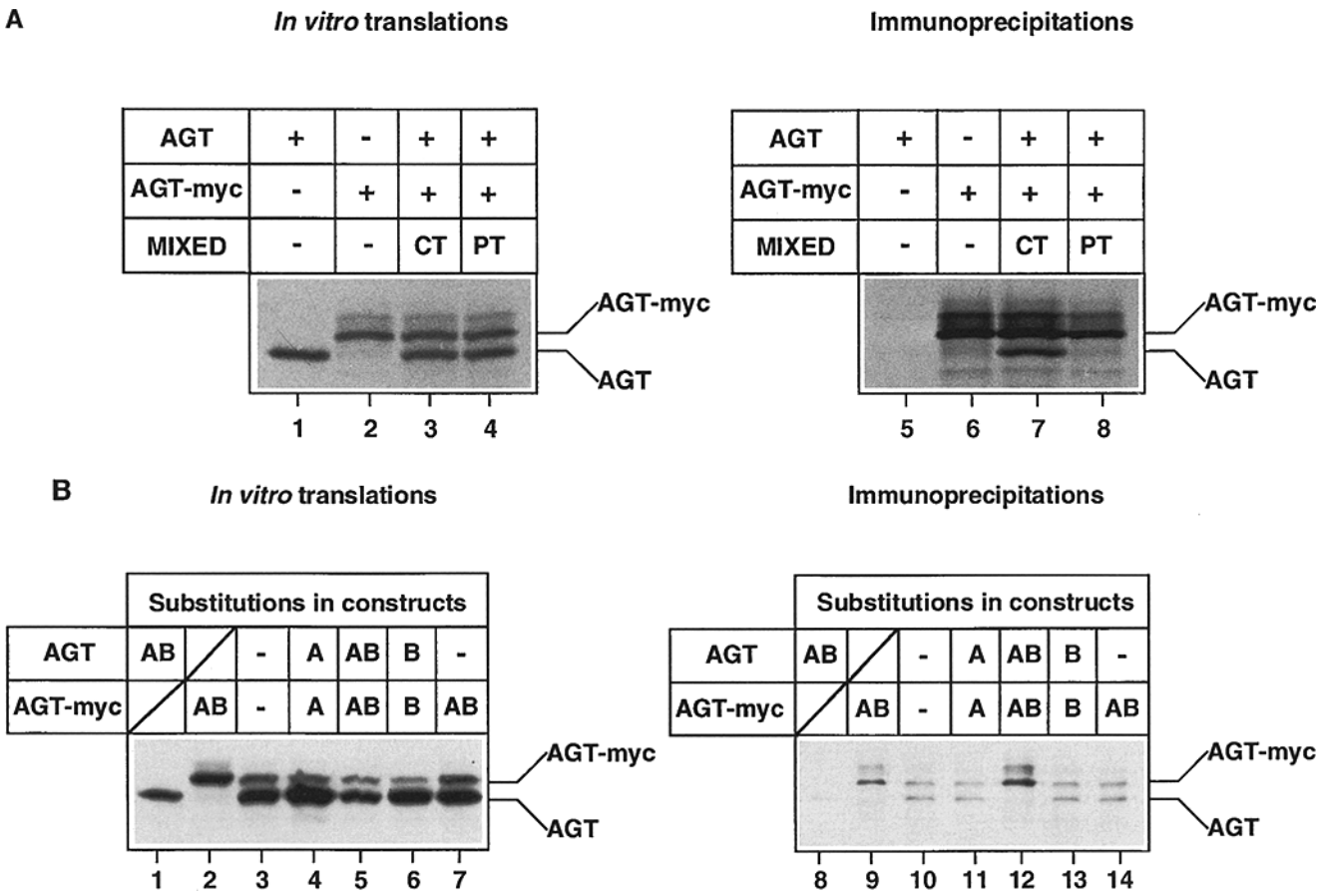

Figure 2. Immunoprecipitation of epitope-tagged AGT. (*A*) Aliquots of in vitro translation reactions, programmed with the transcripts indicated, were either directly resolved by SDS-PAGE on 10% gels (lanes *1–4*) or immunoprecipitated with an anti-myc mAb (lanes *5–8*), and the products were then resolved by SDS-PAGE on 10% gels. In lanes *3* and *8*, AGT and AGT-myc were cotranslated (*CT*), whereas in lanes *4* and *8*, the proteins were translated separately and the products mixed posttranslationally (*PT*). The migration positions of epitope-tagged (*AGT-myc*) and untagged AGT are indicated. (*B*) In vitro translation reactions were programmed with transcripts encoding the various AGTs indicated. After translation, aliquots of reactions were either directly resolved by SDS-PAGE on 10% gels (lanes *1–7*) or immunoprecipitated with an anti-myc mAb and resolved by SDS-PAGE on 10% gels (lanes *8–14*). The migration positions of epitope-tagged (*AGT-myc*) and untagged AGT are indicated. Diagonal lines indicate that a particular construct is not present; dashes indicate that the construct is normal, i.e., it contains neither the A nor B substitutions.

supplemented with 10% FCS at 37°C under 5% CO_2. Cells were split 1:10 on reaching confluence. For electroporation, cells were trypsinized, collected by centrifugation, washed in ice-cold PBSA, and resuspended in PBSA at a concentration of 10^6–10^7 cells/ml. Aliquots of cells (150 μl) were transferred to a 0.4-cm electroporation cuvette (Bio-Rad Laboratories, Richmond, CA), mixed with 50 μl of plasmid DNA (200 μg/ml), and incubated on ice for 10 min. In cotransfection experiments, the myc-tagged AGT DNA to untagged AGT DNA ratio was 1:25, unless otherwise stated. After delivery of a pulse (0.25 kV at 125 μF) in a Bio-Rad gene pulser, the cells were incubated on ice for 10 min. Subsequently, 10^4–10^5 cells were plated in growth medium onto 13-mm glass microscope coverslips. 48 h after transfection, the cells were processed for indirect immunofluorescence microscopy. In some experiments, cells were grown in medium supplemented with 20 μM carbonyl cyanide *m*-chlorophenylhydrazone (CCCP) for 48 h before processing. In many cases, parallel experiments were carried out in which plasmids were transfected into human fibroblasts by intranuclear microinjection essentially as described previously (21).

Immunofluorescence Microscopy

Except when transfected cells were to be double-labeled for AGT and the peroxisomal marker catalase, cells were incubated with 200 nM MitoTracker (Molecular Probes, Cambridge Bioscience, Cambridge, UK) for 15 min at 37°C to label mitochondria. The cells were then washed in PBS and fixed in freshly prepared 3% (wt/vol) paraformaldehyde for 15 min at room temperature. The plasma and peroxisomal membranes were then permeabilized with 1% Triton X-100 for 15 min at room temperature. In some experiments, cells were differentially permeabilized with 25 μg/ml digitonin, instead of Triton X-100, for 5 min at room temperature to selectively permeabilize the plasma membrane. The cells were then processed for single- or double-label indirect immunofluorescence using the following antibodies: rabbit polyclonal anti–human AGT, mouse monoclonal anti-myc (9E10), and rabbit and guinea pig polyclonal anti–human catalase. AGT was visualized with FITC-conjugated goat anti–rabbit IgG (Sigma), and myc was visualized with biotinylated horse anti–mouse IgG and Texas red avidin D or fluorescein streptavidin (Vector Laboratories, Peterborough, UK). Catalase was visualized with either biotinylated goat anti–guinea pig IgG and Texas red avidin D or FITC-conjugated goat anti–rabbit IgG. All incubations were performed at room temperature for 15 min in PBS containing 3% BSA. After each incubation, the cells were washed in PBS. The coverslips were mounted on glass slides in Mowiol (Harlow Chemical Co. Ltd., Harlow, UK) containing diazabicyclo[2,2,2]octane (DABCO, Sigma). The fluorescent staining pattern was viewed in a confocal laser-scanning microscope (MRC 1000; Bio Rad). The captured images were processed using Adobe Photoshop software (Adobe Systems Inc., Mountain View, CA), and were recorded on TMAX 100 ASA B/W film (Eastman Kodak Co., Rochester, NY).

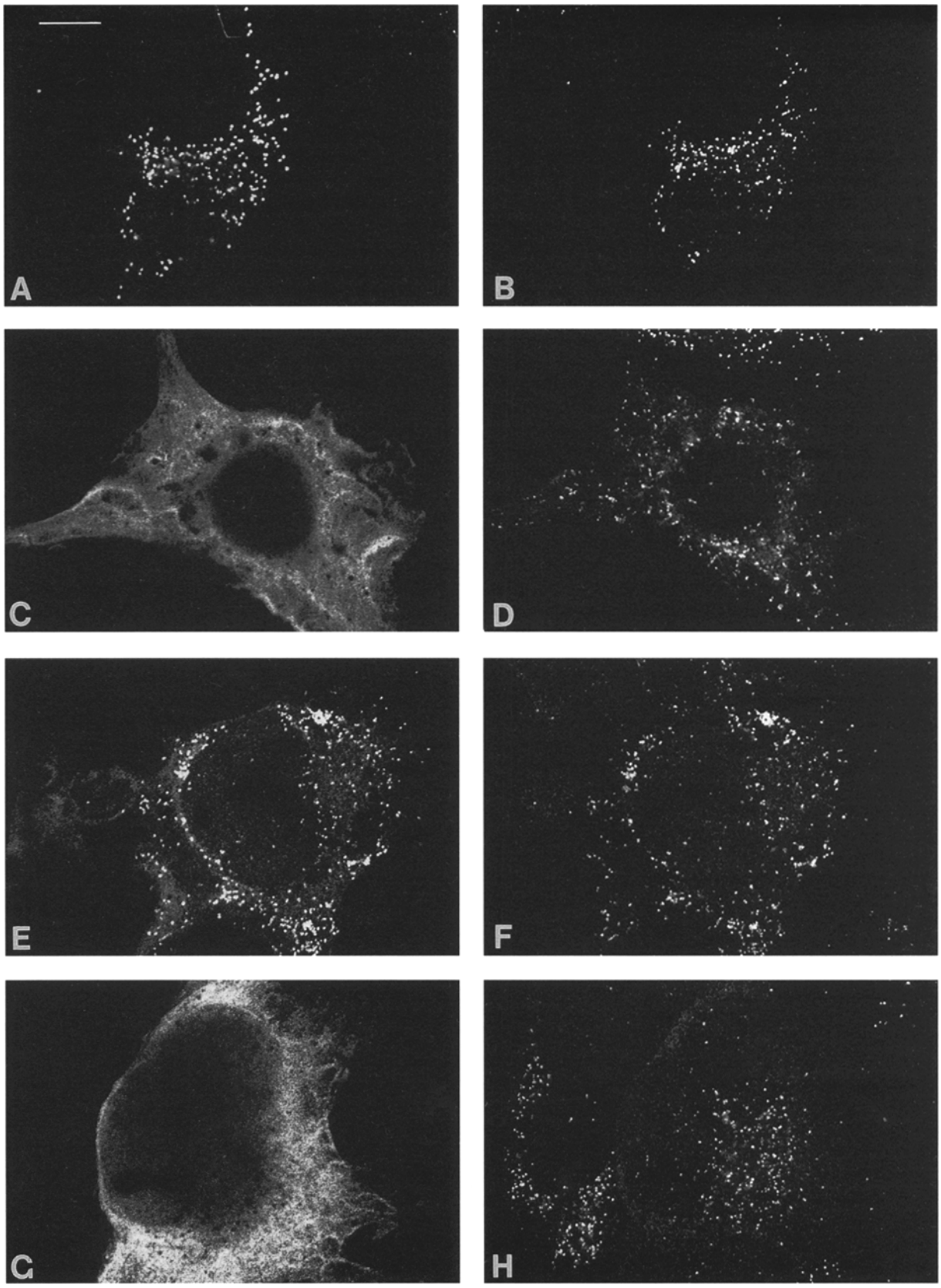

Figure 3. Intracellular localization of AGT and AGT-myc in COS-1 cells. (*A–D*) COS-1 cells transfected with normal AGT (*A* and *B*) or AGT-myc (*C* and *D*) were double labeled for either AGT (*A*) and catalase (*B*) or myc (*C*) and catalase (*D*). (*E–H*) COS-1 cells cotransfected with either AGT-myc and AGT (*E* and *F*) or AGT-myc and AGTΔ1 (*G* and *H*) were double labeled for myc (*E* and *G*) and catalase (*F* and *H*). Bar, 10 μm.

Results

The Combined Presence of $Pro_{11}Leu$ and $Gly_{170}Arg$ Amino Acid Substitutions Inhibit AGT Dimerization In Vitro

AGT purified from a variety of mammalian livers has been shown to exist as a homodimer (34). To test whether AGT translated in vitro is able to dimerize, we examined the oligomeric state of in vitro–translated AGT by chemical cross-linking (Fig. 1). SDS-PAGE of in vitro–translated normal human AGT produced a band of ~43 kD, a size consistent with the predicted molecular mass of monomeric AGT (33). After cross-linking, an additional band of ~90 kD was produced, close to the expected size of dimerized AGT. Since the folding and oligomerization of cytosolic proteins is mediated by molecular chaperones in an ATP-dependent fashion (9), we investigated the effect of ATP depletion (using apyrase) on the posttranslational cross-linking (dimerization) reaction. Posttranslational ATP depletion had no effect on the production of the 90-kD cross-linked product, suggesting that dimerization occurs rapidly in vitro (i.e., before the addition of apyrase). In addition, cross-linking was unaffected by removal of the COOH-terminal PTS1 tripeptide from AGT.

To confirm that the ~90-kD cross-linking product did indeed represent dimerized AGT, we constructed a series of AGT constructs in which the COOH-terminal PTS1 tripeptide was replaced with 12 amino acids containing an epitope tag from c-*myc*. After translation in vitro, myc-tagged normal AGT produced a protein that migrated more slowly than the untagged protein, consistent with the net addition of nine amino acids (Fig. 2 *A*). Normal AGT and AGT-myc were either translated separately, cotranslated, or translated separately and mixed posttranslationally. Translation reactions were subjected to immunoprecipitation with an anti-myc antibody, and aliquots of the initial translation reaction and the immunoprecipitates were resolved by SDS-PAGE (Fig. 2 *A*). When translated alone, untagged normal AGT was not immunoprecipitated by the anti-myc antibody, whereas the AGT-myc was efficiently precipitated (Fig. 2 *A*). When AGT and AGT-myc were cotranslated, untagged AGT was immunoprecipitated. In cotranslations where AGT was in excess over AGT-myc (by ~10-fold), AGT and AGT-myc were coprecipitated in approximately equimolar amounts, confirming that AGT/AGT-myc heterodimers had formed, and that most, if not all, of in vitro–translated AGT does indeed dimerize (Fig. 2 *B*). When the two proteins were translated separately and then mixed posttranslationally, untagged AGT was not coprecipitated with AGT-myc, indicating that once formed, AGT dimers do not readily exchange subunits (Fig. 2 *A*).

To determine the effect of AGT substitutions associated with peroxisome-to-mitochondrion mistargeting in PH1 on AGT dimerization, we performed chemical cross-linking of in vitro–translated AGT encoding various combinations of these substitutions (Fig. 1). Cross-linking of in vitro–translated AGT^{A} and AGT^{B} also produced an ~90-kD product, indicating that neither of these substitutions alone interferes with AGT dimerization in vitro. In contrast, the combined presence of both substitutions in AGT^{AB} completely abolished the production of the ~90-kD band, suggesting that in vitro, these substitutions inhibit AGT dimerization. Similarly, cross-linking of AGT^{ABC} failed to produce a 90-kD product, indicating that the presence of the C substitution does not affect the ability of the A and B substitutions to inhibit AGT dimerization in vitro (data not shown). When epitope-tagged and untagged AGT constructs encoding either the A, the B, or both the A and B substitutions were cotranslated and immunoprecipitated, we observed that either substitution alone did not affect the ability of tagged AGT to coprecipitate untagged AGT (Fig. 2 *B*). Consistent with our chemical cross-linking data, however, the two substitutions together abolished coprecipitation; i.e., AGT^{AB}/AGT^{AB}-myc did not dimerize. However, AGT^{AB}-myc was able to coprecipitate normal AGT (Fig. 2 *B*), AGT^{A} and AGT^{B} (data not shown), indicating that the combined presence of A and B substitutions in both potential subunits is required to inhibit the formation of AGT dimers in vitro.

Normal AGT Is Imported Into Peroxisomes as a Dimer

Our studies of AGT dimerization in vitro raise the possibility that the inhibition of AGT dimerization caused by the combined presence of the A and B substitutions might play a role in the peroxisome-to-mitochondrion mistargeting associated with these substitutions in PH1. To test this hypothesis, we expressed various combinations of myc-tagged and untagged AGT constructs containing either A or B substitutions or both by transfection in COS-1 cells, and determined the intracellular localization of the resulting proteins by immunofluorescence microscopy. When normal AGT was expressed by transfection in COS-1 cells (which do not normally express AGT), it was imported into a particulate compartment that labeled for the peroxisomal marker enzyme catalase (i.e., peroxisomes; Fig. 3, *A* and *B*). In contrast, AGT-myc was dispersed throughout the cytosol, with no apparent evidence of localization to a particulate compartment (Fig. 3, *C* and *D*). These data are consistent with our previous observations that the COOH-terminal tripeptide of AGT is absolutely required for peroxisomal import (21). When AGT-myc was cotransfected with normal AGT (at a ratio of 1:25), however, the myc-tagged protein colocalized with the peroxisomal marker catalase (Fig. 3, *E* and *F*). That AGT-myc had indeed been imported into peroxisomes rather than simply binding to the cytosolic face of the peroxisomal membrane was confirmed by differential digitonin permeabilization of the plasma membrane before immunolabeling (data not shown). Presumably because of heterogeneity in the relative uptake and expression of the AGT and AGT-myc expression plasmids in electroporated COS-1 cells, the distribution of AGT-myc varied widely between individual cotransfected cells. For example, although most cells showed both peroxisomal and cytosolic labeling, in ~10%, it was entirely peroxisomal, and in a few, it was wholly cytosolic. Interestingly, in parallel experiments in which the AGT and AGT-myc expression plasmids were directly injected into the nuclei of human fibroblasts, the distribution of AGT-myc was exclusively peroxisomal in all cells (data not shown). Cotransfection of AGT-myc with AGTΔ1 in COS-1 cells resulted in a cytosolic (diffuse) distribution of AGT-myc,

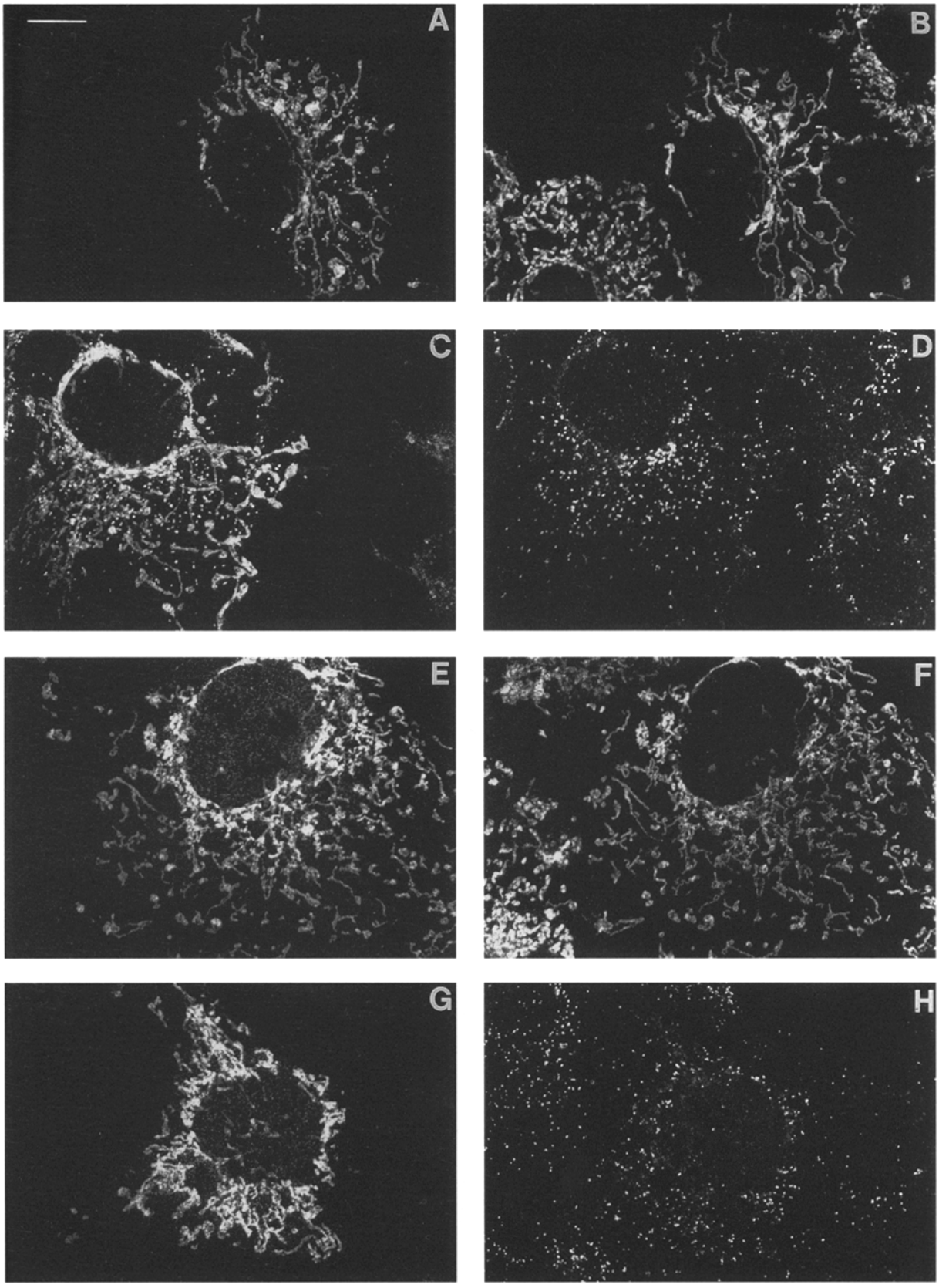

Figure 4. Intracellular localization of mutant AGT in COS-1 cells. (*A–D*) COS-1 cells transfected with AGT^{AB} were double labeled for either AGT (*A*) and MitoTracker (*B*) or AGT (*C*) and catalase (*D*). (*E–H*) Similarly, cells transfected with AGT^{AB}-myc were double labeled for either myc (*E*) and MitoTracker (*F*) or myc (*G*) and catalase (*H*). Bar, 10 μm.

indicating that peroxisomal import of AGT-myc is dependent on an intact PTS in its dimerizing partner (Fig 3, *G* and *H*). Taken together, these data indicate that AGT can be targeted to peroxisomes and committed to peroxisomal import via a PTS1-dependent pathway as a dimer.

Mitochondrial Import of Mutant AGT Is Blocked by Dimerization

Because AGT and AGT^{AB} were able to form heterodimers in vitro, we investigated the ability of AGT to influence the intracellular localization of AGT^{AB}. Consistent with our previous observations (21, 27), when AGT^{AB} was expressed by transfection in COS-1 cells, the protein localized predominantly to the mitochondria, as indicated by its colocalization with the mitochondrial marker MitoTracker (Molecular Probes), although a small but significant proportion localized to peroxisomes (Fig. 4, *A–D*). When AGT^{AB}-myc was expressed in COS-1 cells, the protein was exclusively localized to the mitochondria (Fig 4, *E* and *F*). No localization in the peroxisomes was apparent, presumably because the AGT PTS1 tripeptide has been replaced with the myc epitope in this protein (Fig. 4, *G* and *H*). When AGT^{AB}-myc was coexpressed with normal AGT at a ratio of 1:25, the myc-tagged protein localized to peroxisomes but not to the mitochondria (Fig. 5, *A–D*). Coexpression of AGT^{AB}-myc with AGTΔ1 resulted in a predominantly cytosolic localization of AGT^{AB}myc (Fig. 5, *E* and *F*). These data suggest that AGT^{AB}-myc/AGT dimers form rapidly in the cytosol, and that dimerization makes AGT^{AB}-myc unavailable for mitochondrial import. Furthermore, once AGT^{AB}-myc/AGT dimers have formed, AGT^{AB}-myc does not subsequently become available for mitochondrial import, even in the absence of peroxisomal import.

In contrast to the above, when we coexpressed AGT^{AB}-myc with AGT^{AB}, the myc- tagged protein was exclusively localized to the mitochondria (Fig. 6, *A–D*) even though we showed previously that significant amounts of AGT^{AB} would also be localized in the peroxisomes (Fig. 4, *A–D*). Similar results were obtained when AGT^{ABC} and AGT^{ABC}-myc were coexpressed (data not shown). This is consistent with our in vitro translation data, which indicated that the combined presence of substitutions A and B inhibits AGT homodimerization and that the inhibition of dimerization is not affected by the presence of the C substitution. When we coexpressed AGT^{AB}-myc and AGT^{AB} in COS-1 cells that had been treated with CCCP to inhibit mitochondrial import, however, we observed that a small but significant proportion of myc-tagged protein was imported into peroxisomes, although the majority of the protein remained in the cytosol (Fig. 6, *E* and *F*). Because AGT^{AB}-myc could only be imported into peroxisomes by dimerizing with AGT^{AB}, this observation suggests that in whole cells, the effect of the A and B substitutions is to slow rather than to abolish AGT dimerization. Interestingly, when the mitochondrial import of AGT^{AB} is inhibited by CCCP, the protein is targeted to peroxisomes (Fig. 6 *G*) as efficiently as normal AGT expressed in the presence (Fig. 6 *H*) or absence (Fig. 3 *A*) of CCCP. The small proportion of AGT^{AB}-myc imported into peroxisomes when coexpressed with AGT^{AB} in CCCP-treated cells indicates that only a small proportion dimerizes (with AGT^{AB}). Therefore, provided CCCP does not specifically retard the rate of formation of AGT^{AB}/AGT^{AB}-myc heterodimers (as compared with AGT^{AB}/AGT^{AB} homodimers) or reveal a cryptic PTS within AGT^{AB}-myc, it is probable that the majority of AGT^{AB} is imported into peroxisomes as a monomer. Thus, while normal AGT appears to be imported into peroxisomes as a dimer, dimerization does not appear to be a prerequisite for peroxisomal import.

Both Normal and Mutant AGT Is Dimerized in the Human Liver

To determine the oligomeric status of AGT in human livers, we performed chemical cross-linking of human liver homogenates from a normal individual, in whom AGT is exclusively peroxisomal; a PH1 patient homozygous for A, B, and C substitutions, in whom >90% of AGT is mitochondrial (patient 2 in reference 6, patient G in reference 27); and a panperoxisomal disease patient who was heterozygous for AGT^{A} and AGT, in whom AGT is mainly cytosolic (patient 2 in reference 7, complementation group new and previously unrecognized; Naidu, S., A.B. Moser, C.J. Danpure, L. Civitello, and H.W. Moser, Proceedings of the First Conjoint Meeting of the Child Neurology Society and the International Child Neurology Association, San Francisco, October 2–8, 1994). SDS-PAGE and immunoblotting of liver homogenates from each individual revealed a single immunoreactive band of ~43 kD before cross-linking, which corresponds to the predicted molecular mass of monomeric AGT (Fig. 7, *A–C*). At low cross-linker concentrations in all samples, an additional band of ~90 kD, the expected size of dimerized AGT, was the predominant cross-linked product. However, at higher cross-linker concentrations, the intensity of the ~90-kD band decreased concomitantly with an increase in a band of ~68 kD. While it is possible that the ~68-kD band may be the product of AGT cross-linked to a protein of ~25 kD, its appearance at higher cross-linker concentrations and the associated decrease in the ~90-kD band suggested to us that it more likely represents a more highly cross-linked, and therefore more compact form of dimerized AGT. To investigate this possibility, we performed cross-linking of purified normal human AGT (Fig. 7 *D*). In this preparation, AGT is the only protein visible by silver staining, and in the absence of cross-linker, migrates with an apparent molecular mass of ~43 kD. When cross-linked with low concentrations of cross-linker, the ~43-kD band becomes more diffuse, probably because of intrachain cross-linking, and a band of ~90 kD is produced. At higher cross-linker concentrations, a second cross-linked product of ~68 kD becomes apparent, confirming that both cross-linking products do indeed represent AGT dimers.

These data indicate that despite the presence of substitutions that markedly retard AGT dimerization in vitro in both cellular and noncellular systems, AGT^{AB} can dimerize in human liver mitochondria. It remains to be clarified whether this is caused by the ability of AGT^{AB} to dimerize more efficiently in the mitochondria than in the cytosol, or whether it simply reflects the vastly different time scales involved (0.5–48 h for the in vitro experiments, but probably days to weeks for the PH1 patient). However, prelimi-

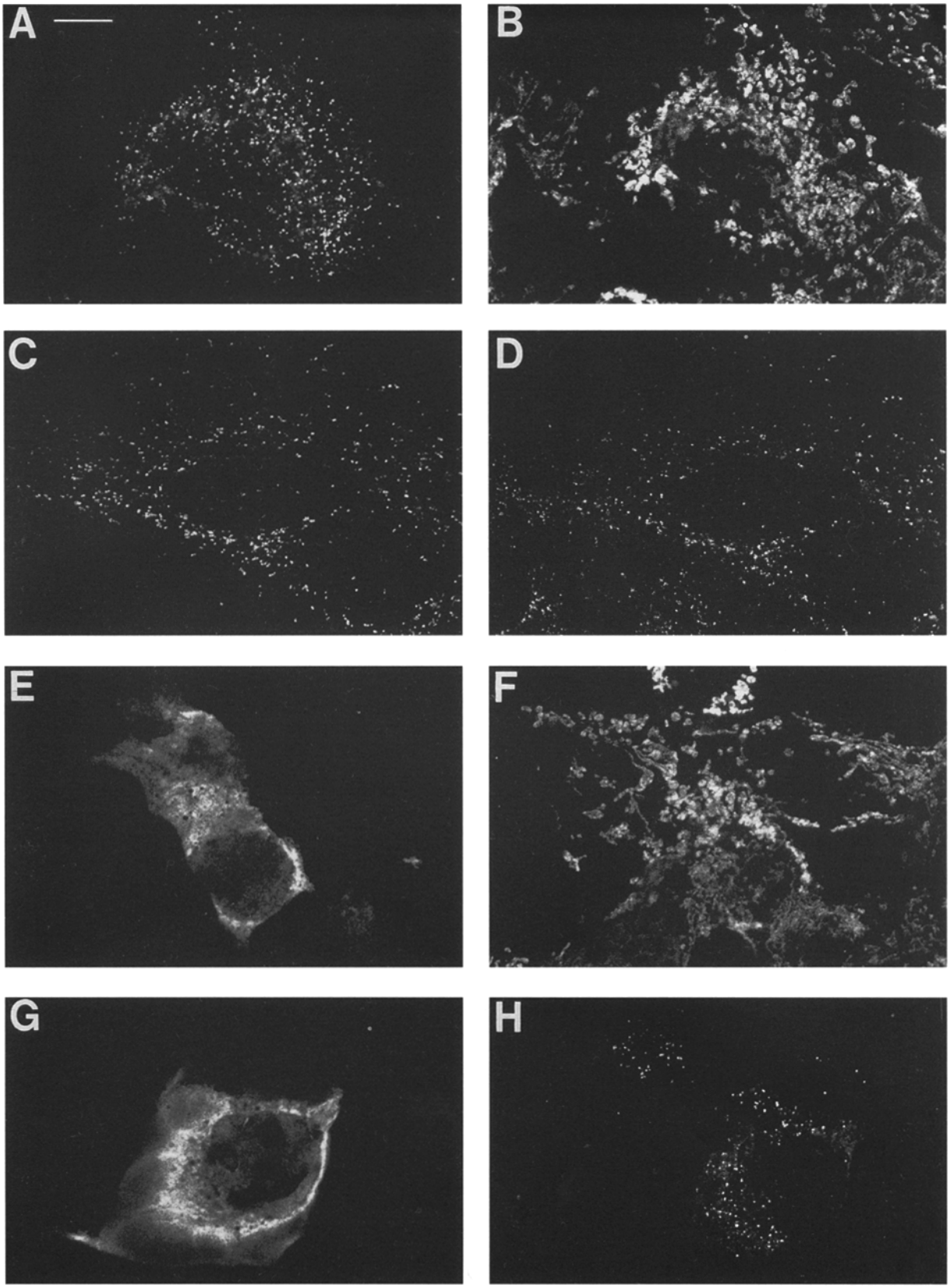

Figure 5. Intracellular localization of mutant AGT in COS-1 cells when coexpressed with normal AGT. COS-1 cells were cotransfected with either AGT^{AB}-myc and normal AGT (*A–D*) or AGT^{AB}-myc and AGTΔ1 (*E–H*). Cells were double labeled for either myc (*A* and *E*) and MitoTracker (*B* and *F*) or myc (*C* and *G*) and catalase (*D* and *H*). Bar, 10 μm.

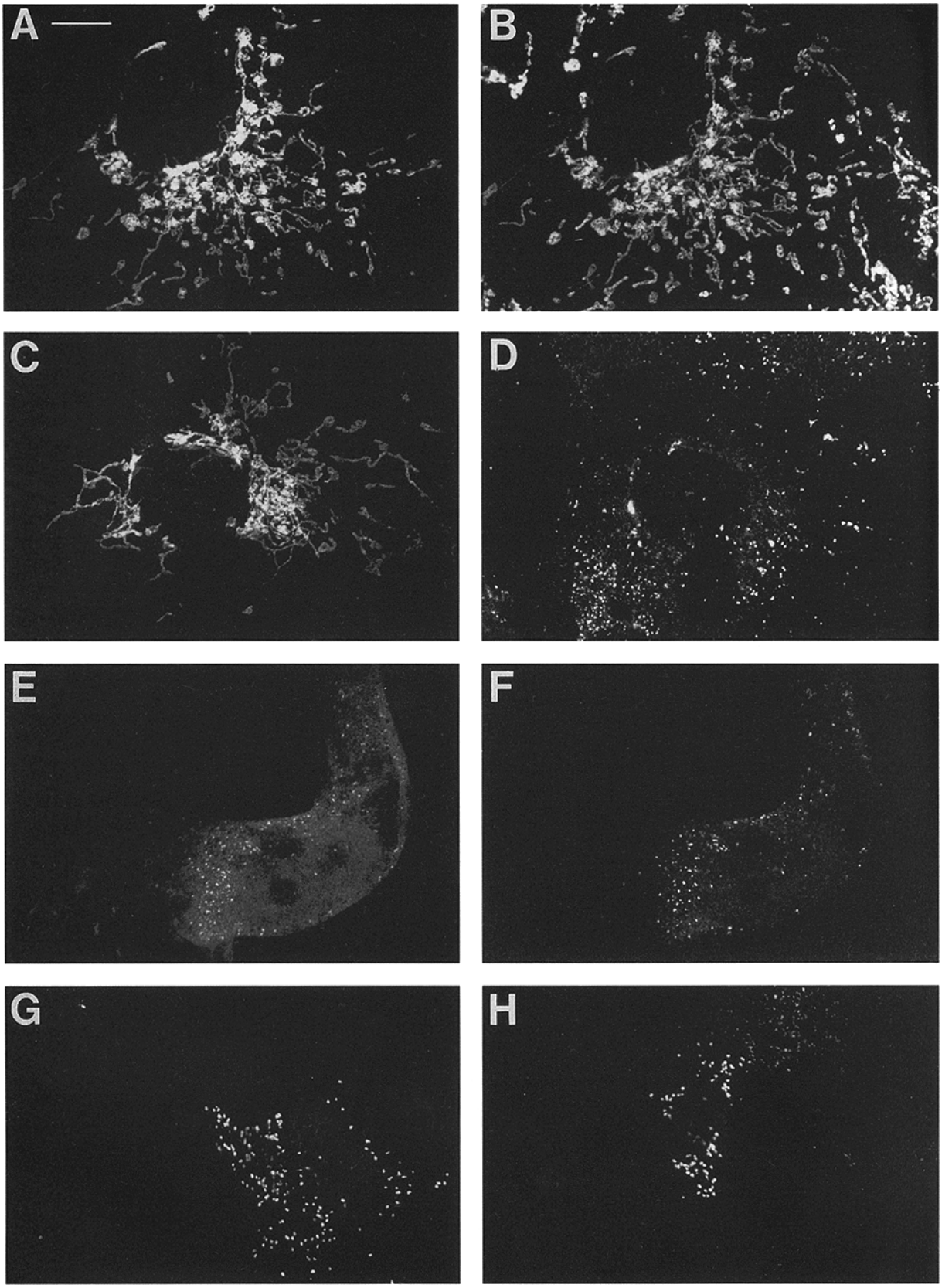

Figure 6. Intracellular localization of mutant AGT in COS-1 cells treated with CCCP. (*A–D*) COS-1 cells were cotransfected with AGT^{AB}-myc and AGT^{AB} and were double labeled for either myc (*A*) and MitoTracker (*B*) or myc (*C*) and catalase (*D*). (*E* and *F*) Cells were cotransfected with AGT^{AB}-myc and AGT^{AB}, cultured in the presence of CCCP, and double labeled for myc (*E*) and catalase (*F*). (*G* and *H*) Cells were transfected with either AGT^{AB} alone (*G*) or normal AGT alone (*H*), cultured in the presence of CCCP, and single labeled for AGT. Bar, 10 μm.

nary studies of the dimerization of AGT^{AB} in transfected COS cells, cultured either in the presence or absence of CCCP, indicate that the rate of dimerization is similar in either the cytosol or the mitochondria. These observations suggest that the differences in AGT^{AB} dimerization in vitro and in vivo reflect differences in time scale rather than organelle-dependent variations in the rate of AGT^{AB} dimerization.

Discussion

The results of the present study, together with previous studies (26, 27), demonstrate that the peroxisome-to-mitochondrion mistargeting of AGT in PH1 is the combined effect of (*a*) the generation of an NH_2-terminal mitochondrial targeting sequence solely caused by the presence of the A substitution; and (*b*) the inhibition of dimerization caused by the presence of both A and B substitutions. These observations are consistent with previous studies of the structural requirements for mitochondrial import, which suggest that oligomerization of proteins inhibits import into the mitochondria. For example, disruption of a domain required for trimerization of a CAT passenger protein has been shown to be required for the in vivo import into mitochondria of an apo-iso-1-cytochrome *c*/CAT fusion (23). Similarly, deletion of an internal segment of the β subunit of mitochondrial F1-ATPase needed for tetramerization has been shown to eliminate the requirement for ATP in in vitro mitochondrial import (4). In a previous study, however, we reported that the A substitution alone was sufficient to direct the import of in vitro–translated AGT into isolated mitochondria (26). How can that data be reconciled with the results of the present study, which indicate that both A and B substitutions are required to inhibit AGT dimerization and thereby allow mitochondrial import? Reexamination of our previous data indicates that the presence of the A substitution alone enables only a small proportion of AGT to be imported into the mitochondria (possibly <10%; 26). It is possible that because of relatively slow protein folding and oligomerization in reticulocyte lysates, a small proportion of AGT molecules remain undimerized. Importantly, in transfected cells, where protein folding and oligomerization might be expected to be more efficient, the A substitution alone is unable to direct the mitochondrial import of detectable levels of AGT (21). Additionally, studies of the intracellular distribution of AGT in an individual homozygous for the A substitution alone indicate that the majority of the protein (>90%) is correctly localized in peroxisomes, although some mistargeting to the mitochondria was clearly detectable (27). Therefore, in whole cells it appears that rapid dimerization excludes all but a few percent of AGT^{A} molecules from the mitochondrial import pathway, despite the presence of an MTS.

The observation that the dimerization of AGT^{AB}-myc with AGTΔ1 can completely block the mitochondrial import of AGT^{AB}-myc suggests that AGT dimerization precedes mitochondrial import in cells, and that once formed, the AGT subunits do not subsequently become available for mitochondrial import. If, as our data indicates, AGT dimerizes rapidly in the cytosol, the question arises as to whether AGT dimers are substrates for peroxisomal import or whether peroxisomal import precedes dimerization. Two pieces of data lead us to conclude that AGT dimers are the substrates for peroxisomal import in whole cells. First, the peroxisomal localization of AGT-myc, when coexpressed with normal AGT, establishes that AGT dimers can at least be committed for peroxisomal import intact. Second, when expressed alone, AGT^{AB} is predominantly localized to mitochondria, suggesting that mitochondrial import precedes peroxisomal import. However, mitochondrial import of AGT^{AB} can be blocked by dimerization with normal AGT. Therefore, dimerization precedes mitochondrial import. One caveat to this argument might be that the combined presence of the A and B substitutions in some way interferes with peroxisomal import. However, this does not seem to be the case because when AGT^{AB} was expressed in cells treated with CCCP, the protein localized exclusively to peroxisomes. Previously, we have shown that neither the A nor B mutation alone interferes with peroxisomal import (21). Although the MTS generated by the A substitution is unusual in that it is not cleaved (26), it is likely that mitochondrial import precedes peroxisomal import, even when a normal MTS is present. For example, recent studies have shown that in feline AGT, which contains a classical cleavable mitochondrial targeting presequence, mitochondrial import takes precedence over peroxisomal import (23a). In such a case, it appears that the presence of the MTS itself inhibits AGT dimerization (our unpublished observations).

Early studies of the kinetics of peroxisomal protein oligomerization and import supported a model of protein translocation in which proteins were imported in a monomeric state and subsequently oligomerized in the peroxisomal matrix. Thus, de Duve and Lazarow (15, 16) showed that in whole-liver pulse chase experiments, catalase monomers associated with peroxisomes in vivo before being converted to tetramers. Similarly, Goodman et al. (11) demonstrated that the kinetics of oligomerization and peroxisomal import of alcohol oxidase, an octameric flavoprotein from *Candida boidinii*, were similar, a finding that was interpreted as indicating that monomers are translocated into peroxisomes, where they then octamerize.

More recently, however, several new lines of evidence have required a reevaluation of this model. First, cell fusion of fibroblasts from complementary Zellweger lines indicated that a preexisting pool of cytosolic, tetrameric catalase could be translocated into newly generated peroxisomes that are produced upon fusion (2). Second, studies of the oligomerization of catalase in normal human fibroblasts using conformation-specific antibodies have suggested that catalase assembles into a tetramer in the cytosol before becoming associated with peroxisomes (20). These data are apparently at variance with earlier reports that indicated that the import of catalase was inhibited by aminotriazole, a compound that covalently binds to and inhibits catalase (19). In this study, it was suggested that binding of aminotriazole might inhibit peroxisomal import by preventing the dissociation of catalase subunits. An alternative interpretation of these data, however, might be that aminotriazole exerts its effect by binding to and in some way obscuring specific targeting sequences within catalase.

The third and by far the most persuasive piece of evidence supporting a model of oligomeric protein import

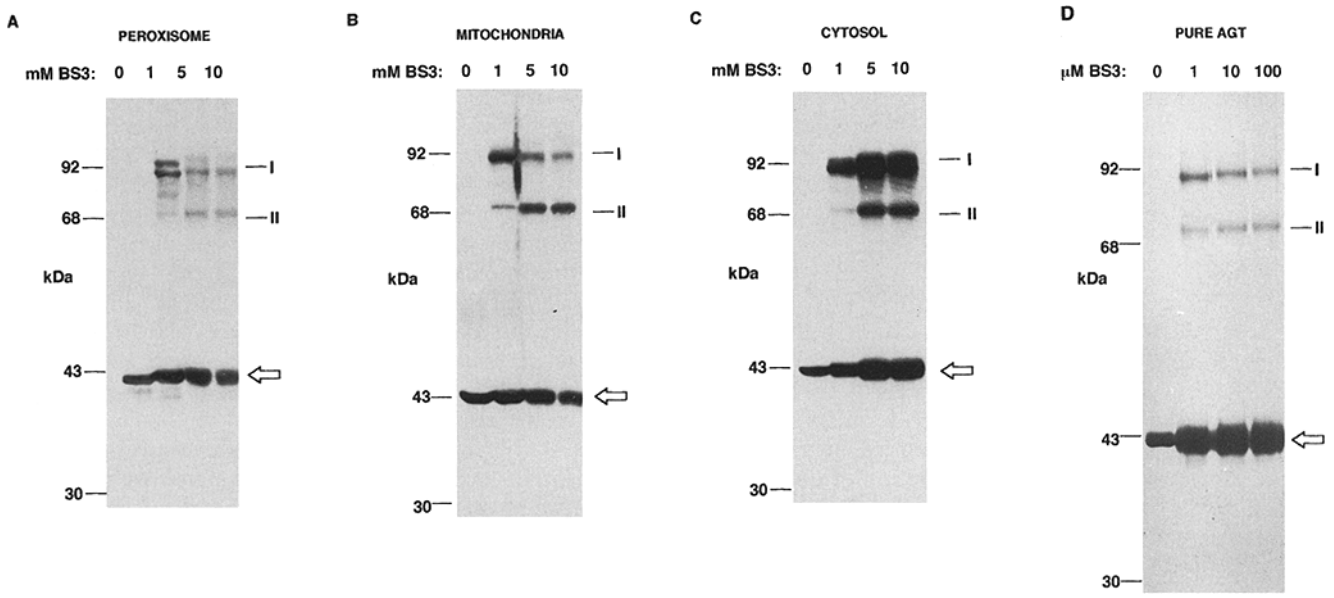

Figure 7. Chemical cross-linking of human liver AGT. (*A–C*) Postnuclear supernatants of human liver homogenates from a normal individual in which AGT was entirely peroxisomal (*PEROXISOME*), a PH1 patient in which AGT was >90% mitochondrial (*MITOCHONDRIA*), and a panperoxisome disease patient in whom AGT was entirely cytosolic (*CYTOSOL*) were cross-linked with increasing concentrations of the cross-linker BS3, as indicated. After cross-linking, proteins were resolved by SDS-PAGE on either 10% (*A* and *B*) or 12% (*C*) SDS-PAGE gels and transferred to nitrocellulose membranes. AGT was visualized by immunoblotting with rabbit anti–human AGT polyclonal serum followed by ECL. The migration positions of monomeric AGT (*open arrow*) and the two major cross-linking products (*I* and *II*) are indicated. (*D*) Normal human AGT was purified essentially as previously described (35). Aliquots of the purified protein were cross-linked with increasing concentrations of the cross-linker BS3, as indicated. After cross-linking, proteins were resolved by SDS-PAGE on 12% gels and visualized by silver staining. The migration positions of monomeric AGT (*open arrow*) and the two major cross-linking products (*I* and *II*) are indicated. The positions of the molecular mass markers (in kilodaltons) are shown on the left-hand side of each gel. At the present time, we have no explanation for the higher cross-linking efficiency of cytosolic AGT (*C*) than peroxisomal (*A*) or mitochondrial (*B*) AGT. We consider that it is unlikely to be related to the genotype of this individual, who is heterozygous for the A mutation (7), since this mutation had no effect on AGT dimerization in vitro (see Fig. 1). We also think that it is unlikely to be related to the accessibility of the cross-linker to AGT in the homogenates, since the liver samples were frozen and thawed before homogenization. Irrespective of this, it is clear that AGT^{AB} (*B*) can dimerize in vivo.

into peroxisomes comes from studies of both PTS1 and PTS2 import pathways in the yeast *S. cerevisiae.* Thus, McNew and Goodman (18) demonstrated that the trimeric bacterial protein CAT, fused to a COOH-terminal PTS1-bearing peptide, is imported into yeast peroxisomes. When the rates of trimerization and peroxisomal import were determined, trimerization clearly preceded import. In similar studies, Glover et al. (10) examined the dimerization and import of thiolase, a PTS2 containing protein. A mutant form of thiolase from which the PTS2 had been deleted was imported into peroxisomes only when coexpressed with normal thiolase, suggesting that in yeast, oligomeric protein import may extend to both PTS1 and PTS2 pathways. A clear demonstration that macromolecular structures (whether monomers or oligomers) can be imported into peroxisomes has been provided by the work of Walton and colleagues (37). These authors have examined the import competence of a number of artificial peroxisomal substrates ranging from HSA to 9-nm gold particles by microinjection into fibroblasts. When conjugated to numerous 12–amino acid peptides that terminate with the PTS1 tripeptide SKL, HSA was imported into peroxisomes. Chemical cross-linking of the albumin moiety, to prevent unfolding before import, did not inhibit import, suggesting that highly folded molecules can be translocated across the peroxisomal membrane. This suggestion was strengthened by the finding that 9-nm gold particles coated with the HSA-peptide conjugates were also imported into peroxisomes.

The unparalleled peroxisome-to-mitochondrion mistargeting of AGT in PH1 has provided a unique opportunity to compare and contrast the structural requirements for protein import into these two organelles. The results presented in this paper provide the first evidence for the oligomeric peroxisomal import of a naturally occurring PTS1 protein, and they demonstrate a novel mechanism by which enzyme mistargeting can lead to a lethal human hereditary disease.

The work described in this paper was supported by a United Kingdom Medical Research Council Programme grant (9215074) to C.J. Danpure.

Received for publication 28 June 1996 and in revised form 28 August 1996.

References

1. Attardi, G., and G. Schatz. 1988. Biogenesis of mitochondria. *Annu. Rev. Cell Biol.* 4:289–333.
2. Brul, S., E.A. Wiemer, A. Westerveld, A. Strijland, R.J. Wanders, A.W. Schram, H.S. Heymans, R.B. Schutgens, H. van den Bosch, and J.M. Tager. 1988. Kinetics of the assembly of peroxisomes after fusion of complementary cell lines from patients with the cerebro-hepato-renal (Zell-

weger) syndrome and related disorders. *Biochem. Biophys. Res. Commun.* 152:1083–1089.
3. Chen, W.J., and M.G. Douglas. 1987. The role of protein structure in the mitochondrial import pathway. Unfolding of mitochondrially bound precursors is required for membrane translocation. *J. Biol. Chem.* 262: 15605–15609.
4. Chen, W.J., and M.G. Douglas. 1988. An F1-ATPase beta-subunit precursor lacking an internal tetramer-forming domain is imported into mitochondria in the absence of ATP. *J. Biol. Chem.* 263:4997–5000.
5. Cooper, P.J., C.J. Danpure, P.J. Wise, and K.M. Guttridge. 1988. Immunocytochemical localization of human hepatic alanine:glyoxylate aminotransferase in control subjects and patients with primary hyperoxaluria type 1. *J. Histochem. Cytochem.* 36:1285–1294.
6. Danpure, C.J., P.J. Cooper, P.J. Wise, and P.R. Jennings. 1989. An enzyme trafficking defect in two patients with primary hyperoxaluria type 1: peroxisomal alanine/glyoxylate aminotransferase rerouted to mitochondria. *J. Cell Biol.* 108:1345–1352.
7. Danpure, C.J., P. Fryer, S. Griffiths, K.M. Guttridge, P.R. Jennings, J. Allsop, A.B. Moser, S. Naidu, H.W. Moser, M. MacCollin, and D.C. DeVivo. 1994. Cytosolic compartmentalization of hepatic alanine:glyoxylate aminotransferase in patients with aberrant peroxisomal biogenesis and its effect on oxalate metabolism. *J. Inher. Metab. Dis.* 17:27–40.
8. Eilers, M., and G. Schatz. 1988. Protein unfolding and the energetics of protein translocation across biological membranes. *Cell.* 52:481–483.
9. Frydman, J., E. Nimmesgern, K. Ohtsuka, and F.U. Hartl. 1994. Folding of nascent polypeptide chains in a high molecular mass assembly with molecular chaperones. *Nature (Lond.).* 370:111–117.
10. Glover, J.R., D.W. Andrews, and R.A. Rachubinski. 1994. *Saccharomyces cerevisiae* peroxisomal thiolase is imported as a dimer. *Proc. Natl. Acad. Sci. USA.* 91:10541–10545.
11. Goodman, J.M., C.W. Scott, P.N. Donahue, and J.P. Atherton. 1984. Alcohol oxidase assembles post-translationally into the peroxisome of *Candida boidinii*. *J. Biol. Chem.* 259:8485–8493.
12. Gould, S.J., G.A. Keller, N. Hosken, J. Wilkinson, and S. Subramani. 1989. A conserved tripeptide sorts proteins to peroxisomes. *J. Cell Biol.* 108: 1657–1664.
13. Hartl, F.U., N. Pfanner, D.W. Nicholson, and W. Neupert. 1989. Mitochondrial protein import. *Biochim. Biophys. Acta.* 988:1–45.
14. Hendrick, J.P., T. Langer, T.A. Davis, F.U. Hartl, and M. Wiedmann. 1993. Control of folding and membrane translocation by binding of the chaperone DnaJ to nascent polypeptides. *Proc. Natl. Acad. Sci. USA.* 90:10216–10220.
15. Lazarow, P.B., and C. De Duve. 1973. The synthesis and turnover of rat liver peroxisomes. V. Intracellular pathway of catalase synthesis. *J. Cell Biol.* 59:507–524.
16. Lazarow, P.B., and C. De Duve. 1973. The synthesis and turnover of rat liver peroxisomes. IV. Biochemical pathway of catalase synthesis. *J. Cell Biol.* 59:491–506.
17. Lazarow, P.B., and Y. Fujiki. 1985. Biogenesis of peroxisomes. *Annu. Rev. Cell Biol.* 1:489–530.
18. McNew, J.A., and J.M. Goodman. 1994. An oligomeric protein is imported into peroxisomes in vivo. *J. Cell Biol.* 127:1245–1257.
19. Middelkoop, E., A. Strijland, and J.M. Tager. 1991. Does aminotriazole inhibit import of catalase into peroxisomes by retarding unfolding? *FEBS Lett.* 279:79–82.
20. Middelkoop, E., E.A. Wiemer, D.E. Schoenmaker, A. Strijland, and J.M. Tager. 1993. Topology of catalase assembly in human skin fibroblasts. *Biochim. Biophys. Acta.* 1220:15–20.
21. Motley, A., M.J. Lumb, P.B. Oatey, P.R. Jennings, P.A. De Zoysa, R.J. Wanders, H.F. Tabak, and C.J. Danpure. 1995. Mammalian alanine:glyoxylate aminotransferase 1 is imported into peroxisomes via the PTS1 translocation pathway. Increased degeneracy and context specificity of the mammalian PTS1 motif and implications for the peroxisome-to-mitochondrion mistargeting of AGT in primary hyperoxaluria type 1. *J. Cell Biol.* 131:95–109.
22. Noguchi, T., and Y. Takada. 1979. Peroxisomal localization of alanine:glyoxylate aminotransferase in human liver. *Arch. Biochem. Biophys.* 196: 645–647.
23. Nye, S.H., and R.C. Scarpulla. 1990. Mitochondrial targeting of yeast apoiso-1-cytochrome *c* is mediated through functionally independent structural domains. *Mol. Cell Biol.* 10:5763–5771.
23a. Oatey, P.B., M.J. Lumb, and C.J. Danpure. 1996. Molecular basis of the variable mitochondrial and peroxisomal localisation of alanine: glyoxylate aminotransferase. *Eur J. Biochem.* In press.
24. Osumi, T., T. Tsukamoto, S. Hata, S. Yokota, S. Miura, Y. Fujiki, M. Hijikata, S. Miyazawa, and T. Hashimoto. 1991. Amino-terminal presequence of the precursor of peroxisomal 3-ketoacyl-CoA thiolase is a cleavable signal peptide for peroxisomal targeting. *Biochem. Biophys. Res. Commun.* 181:947–954.
25. Pfanner, N., and W. Neupert. 1990. The mitochondrial protein import apparatus. *Annu. Rev. Biochem.* 59:331–353.
26. Purdue, P.E., J. Allsop, G. Isaya, L.E. Rosenberg, and C.J. Danpure. 1991. Mistargeting of peroxisomal L-alanine:glyoxylate aminotransferase to mitochondria in primary hyperoxaluria patients depends upon activation of a cryptic mitochondrial targeting sequence by a point mutation. *Proc. Natl. Acad. Sci. USA.* 88:10900–10904.
27. Purdue, P.E., Y. Takada, and C.J. Danpure. 1990. Identification of mutations associated with peroxisome-to-mitochondrion mistargeting of alanine/glyoxylate aminotransferase in primary hyperoxaluria type 1. *J. Cell Biol.* 111:2341–2351.
28. Roise, D., and G. Schatz. 1988. Mitochondrial presequences. Minireview. *J. Biol. Chem.* 263:4509–4511.
29. Schleyer, M., and W. Neupert. 1985. Transport of proteins into mitochondria: translocational intermediates spanning contact sites between outer and inner membranes. *Cell.* 43:339–350.
30. Subramani, S. 1993. Protein import into peroxisomes and biogenesis of the organelle. *Annu. Rev. Cell Biol.* 9:445–478.
31. Swinkels, B.W., S.J. Gould, A.G. Bodnar, R.A. Rachubinski, and S. Subramani. 1991. A novel, cleavable peroxisomal targeting signal at the amino-terminus of the rat 3-ketoacyl-CoA thiolase. *EMBO (Eur. Mol. Biol. Organ.) J.* 10:3255–3262.
32. Swinkels, B.W., S.J. Gould, and S. Subramani. 1992. Targeting efficiencies of various permutations of the consensus COOH-terminal tripeptide peroxisomal targeting signal. *FEBS Lett.* 305:133–136.
33. Takada, Y., N. Kaneko, H. Esumi, P.E. Purdue, and C.J. Danpure. 1990. Human peroxisomal L-alanine:glyoxylate aminotransferase. Evolutionary loss of a mitochondrial targeting signal by point mutation of the initiation codon. *Biochem. J.* 268:517–520.
34. Takada, Y., and T. Noguchi. 1982. Subcellular distribution, and physical and immunological properties of hepatic alanine:glyoxylate aminotransferase isoenzymes in different mammalian species. *Comp. Biochem. Physiol. (B).* 72:597–604.
35. Thompson, J.S., and K.E. Richardson. 1967. Isolation and characterization of an L-alanine:glyoxylate aminotransferase from human liver. *J. Biol. Chem.* 242:3614–3619.
36. von Heijne, G. 1986. Mitochondrial targeting sequences may form amphiphilic helices. *EMBO (Eur. Mol. Biol. Organ.) J.* 5:1335–1342.
37. Walton, P.A., P.E. Hill, and S. Subramani. 1995. Import of stably folded proteins into peroxisomes. *Mol. Biol. Cell.* 6:675–683.